UNIVERSITY OF CALIFORNIA, SAN DIEGO

The localization of naive and memory $CD8^+$ T cells following infection

A thesis submitted in partial satisfaction of the requirements for the degree of Master of Science

in

Biology

by

Edward Yang

Committee in charge:

Professor Ananda W. Goldrath, Chair
Professor Colin Jamora
Professor Elina Zuñiga

2009

The thesis of Edward Yang is approved and it is acceptable in quality and form for publication on microfilm and electronically:

Chair

University of California, San Diego

2009

TABLE OF CONTENTS

LIST OF FIGURES

ACKNOWLEDGEMENTS

Figures 3-8, in full, are reprints of the material as they appears in a manuscript currently in review at The Journal of Immunology, with the running title "Memory-like $CD8^+$ T cells generated during homeostatic proliferation defer to antigen-experienced memory cells." Authors are as follows: Kitty P. Cheung, Edward Yang, and Ananda W. Goldrath. The thesis author was the second author of this paper.

First and foremost, I would like to thank Ananda for taking me as one of her students and allowing me the priceless experiences I've received these past two years. You have been an incredible mentor, whether it is pushing me to think, helping me in every situation, acquainting me with delicious varieties of food, or enlightening my views on life. I know that in these past two years, I've grown more than I have in the past decade, and without you, I would not have had the opportunity to do so. Kitty, my mentor too and friend, what I have accomplished would have been impossible without your guidance. From day one you were always patient in teaching me every technique that I know, whether it's something you've done a million times or a new protocol neither of us have tried. I've really enjoyed working with you; it makes coming into lab not a chore but part of my day that I look forward to. Thank you. Adam, I don't even know where to start about the countless discussions we've had on nearly "everything", whether it be the latest rumors about the next iPhone, which dim sum place tastes the best, and, yes, repeatedly asking you about the mystery surrounding KLRG-1. I learn something new every day. Cliff Yang, my Chinese brother from another mother and father, thanks for the laughs, and helping me connect with my asian roots. Louise, thanks for always listening and discussing when I have any scientific question, and of course, for keeping my eating

habits in check. Mark, you've helped direct me in many of my questions and experiments, and thanks for the massive amounts of GM-CSF. Jamie, it may not seem like it, but I've definitely learned something with your repeated reminders about cleaning my bench. Jessica, I've gotten to know you pretty well in the past year, and I want to thank you for always holding very lively conversations with me on nearly everything. Andrew, you've provided me with a lot of good insight on presenting myself in various formal situations, from interviews to talks. Colin, starting out with Cell Biology Lab and beyond – I honestly did learn so much from you (as much as I dreaded those exams). You are unforgettable, and I always enjoy seeing you when I come to sixth floor. And, of course, thank you for letting me use the cryostat. My thesis would not be here today without it. Pedro, you too are unforgettable man. Whether it's teaching me all that I know about histology, berating me about, well, being Ed, or discussing the different insightful aspects of life, you've been a big part of my life these past years.

Since my first few days with the Goldrath lab, I know Kitty won't forget me after the inappropriate choice for the print on my "that" shirt. It's really been an amazing two years in the Goldrath lab. Not only have I been trained to think much more critically, I've already learned more than I had ever imagined about immunology, as well as enjoying the exquisite delicacies of fine culinary… for lack of a better word… concoctions. My time in this lab has been a blessing that I truly can never forget.

ABSTRACT OF THE THESIS

The localization of naive and memory CD8$^+$ T cells following infection

by

Edward Yang

Master of Science in Biology

University of California, San Diego, 2009

Professor Ananda W. Goldrath, Chair

Different subsets of memory CD8$^+$ T cells populate the T cell compartment. Antigen-experienced memory (true-memory) cells are formed in a classic immune response against an invading pathogen, but memory-like (HP-memory) cells can also be generated through antigen-independent homeostatic proliferation resulting from lymphopenia. HP-memory cells subsequently acquire the same effector functions and surface marker expression as true-memory cells. When HP- and true-memory CD8$^+$ cells of the same specificity compete in conditions of infection, true-memory cells expand to a greater degree and form more secondary memory. Here, we found that HP- and true-

memory cells demonstrated aberrant chemokine receptor expression and distinct localization within the spleen during infection, indicating differential access to signals necessary for secondary memory formation.

Interestingly, we discovered in subsequent experiments that naïve $CD8^+$ T cells display strikingly similar localization patterns to that of HP-memory cells. In the late phase immune response, true-memory $CD8^+$ T cells are nearly absent from the splenic T cell zones, while a significant population of naïve or HP-memory subsets are retained in the PALS. As dendritic cells are crucial in providing activation, co-stimulatory, and memory differentiation signals to $CD8^+$ T cell, we analyzed colocalization of T cells and DCs over the course of the immune response. In summary, HP-memory T cells provide protection without compromising the true-memory population, and the differential localization patterns among naïve, HP-, and true-memory cells in relation to DCs suggest that these cell types may influence their ability to compete and form a memory population.

INTRODUCTION

The immune response and memory

The adaptive immune system mediates recognition of virtually any non-self organism or molecular structure and mediates the hallmark feature of immunological memory. The concept of immunological memory is an intrinsic characteristic of the immune system that confers lasting and effective protection upon re-exposure to a pathogen. There are B and T cell compartments within the adaptive immune system, and $CD8^+$ T cells constitute an indispensable wing of the immune response. Without $CD8^+$ T cells, the ability to clear many intracellular infections is virtually ablated.

In uninfected individuals, naïve $CD8^+$ T cells circulate throughout the body and survey the antigen presenting cells (APCs) in secondary lymphoid organs for their target antigen [1]. These naïve $CD8^+$ T cells survive through signals from self-MHC-I:peptide interactions and interleukin-7 (IL-7) [2] and can be identified by distinct expression of an array of cell surface makers [1].

During initial encounter with a pathogen, the immune system selectively expands antigen-specific naïve $CD8^+$ T cells into an army of immune cells tailored to eliminate the invading pathogen. For this process to occur, APCs must present the antigen to antigen-specific $CD8^+$ T cells. Upon encounter with a mature APC presenting the cognate peptide:MHC-I complex in the presence of sufficient costimulatory signals, naïve $CD8^+$ T cells will transition into phases of short and long interactions with APCs that eventually lead to the first phase of the immune response, clonal selection and expansion [3]. Though the process takes three to five days, these events prompt the activation and

extensive proliferation of naïve $CD8^+$ T cells into mass armies of antigen-specific effector cells, in the process acquiring effector functions including production of perforin and granzyme, secretion of cytokines such as IL-2 and IFN-gamma, and modification of homing signature [4-10].

The job of these effector $CD8^+$ T cells is to eliminate the pathogen, and upon completing this task, will undergo widespread apoptosis in the second phase of the immune response, contraction. As there is limited space in the secondary lymphoid compartment, expanded effector cells must undergo contraction in order to comply with these constraints that govern T cell homeostasis [2, 11-13]. Either way, the contraction phase is followed by the third and last stage, the formation of stable memory cells [7, 8]. The few lymphocytes that fail to undergo contraction remain to establish immunological memory, the ability to rapidly initiate a robust response against subsequent encounters with the target pathogen, bypassing the initial lengthy process of activation and clonal selection. It is important to note that these are naïve T cells that have been programmed into memory (true-memory) cells due to antigenic exposure. Surprisingly, cells with the phenotypic and functional qualities of memory cells can also be generated in the absence of antigen in response to lymphopenic environments.

In uninfected, wildtype mice, the immune compartment can be considered “full” in the sense that there is an equilibrium between numbers of competing T cells and finite survival signals, such as IL-7 and IL-15 [13]. Thus, the T cell compartment can only consistently maintain a fixed range of T lymphocytes numbers. In contrast, there are also states of lymphopenia, the lack of lymphocytes, where the overabundance of such signals due to diminished competition can induce homeostatic proliferation and differentiation of

naïve $CD8^+$ T cells into a memory-like (HP-memory) state without exposure to antigen [13-17].

HP- and true-memory $CD8^+$ T cells both function to rapidly initiate robust immune responses upon exposure to the target antigen. It is therefore of interest in this thesis to determine the effects of competition among these memory subsets and the profile of their individual responses. The hallmark of our immune systems is the ability to establish immunological memory, but even after decades of debate, the mechanism of transition and formation into this state from the primary immune response remains obscure. This key aspect of our immune systems defines not only our protection against future pathogens, but also is relevant to progress in fields such as vaccine design, allergy, autoimmunity, chemotherapy, cancer therapy, etc.

Anatomy of the spleen

When visualizing the immune response, it is important to note the anatomical structure of the spleen. The spleen is a secondary lymphoid organ that sits above the stomach (Fig. 1). It functions to not only allow B and T lymphocytes to survey the blood for pathogens, but also to remove aging red blood cells. The microanatomy within the spleen is organized into red and white pulp. The red pulp generally contains red blood cells and networks of blood vessels, but the white pulp is more highly structured. Within each white pulp, there is a B cell zone and a T cell zone, also known as the periarteriolar lymphoid sheath (PALS) (Fig. 1). Together, the structure of the spleen allows efficient coordination of the adaptive immune system with the rest of the body upon infection with a pathogen.

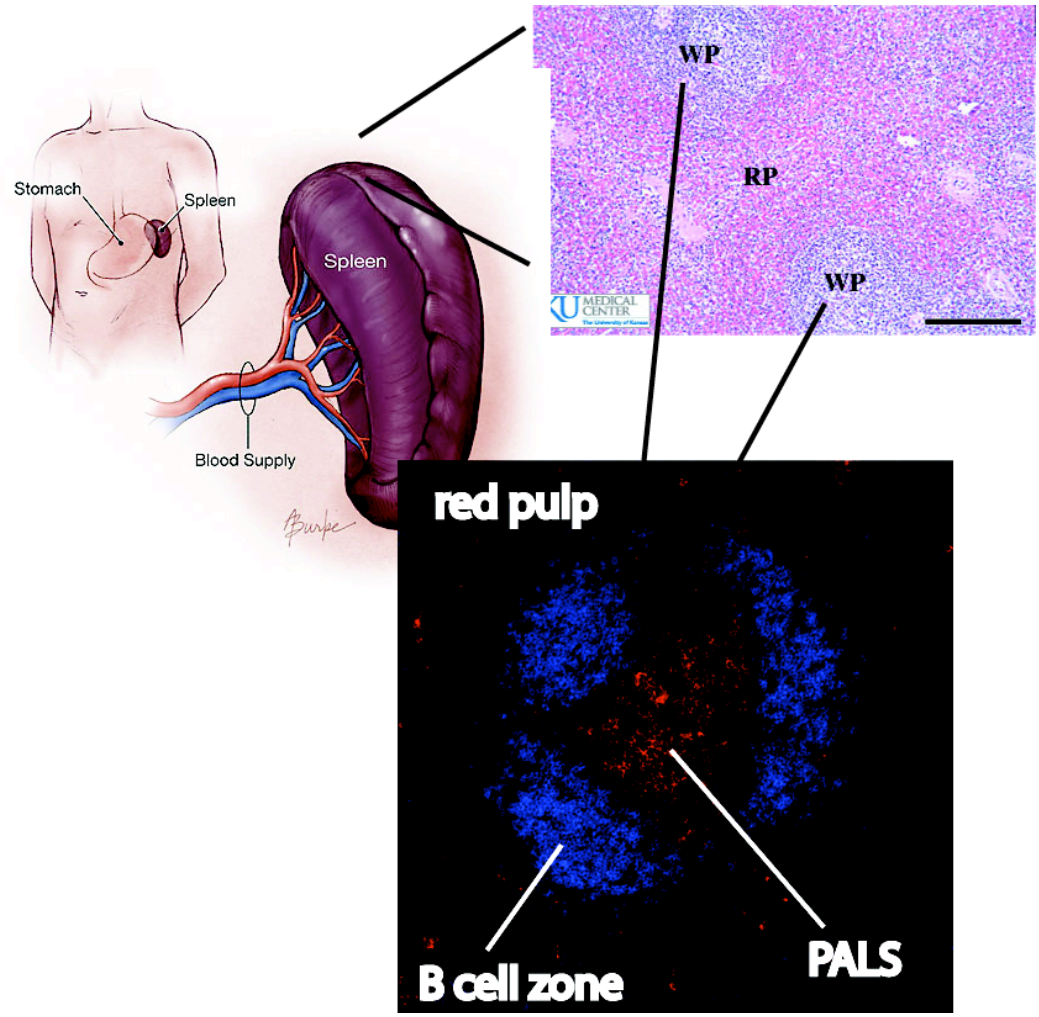

Figure 1: Anatomy of the spleen
Images depicting the anatomy and microanatomy of the spleen. B cells are blue and T cells are red. Images courtesy of http://www.medem.com and http://www.kumc.edu.

The role of dendritic cells

Upon infection, APCs initiate T cell expansion and interface with B cells and the innate immune system. Of note, dendritic cells (DCs) are thought to be the most crucial type of APC for activating and programming $CD8^+$ T cells into memory cells [18]. Previous experiments have shown that DCs are essential in inducing naïve $CD8^+$ T cells to activate and proliferate [19]. Even though peptide-loaded macrophages are also

capable of initiating a $CD8^+$ T cell response [20], deletion of DCs results in the lack of $CD8^+$ T cell priming and subsequent expansion [19].

DCs acquire and cross-present the antigen to $CD8^+$ T cells. Binding of the T cell receptor to MHC:peptide complexes on DCs, in the context of proper co-stimulation and cytokine signals, activate naïve $CD8^+$ T cells. It is thought that the site of T cell priming in the spleen is the periarteriolar lymphoid sheath (PALS), also known as the T cell zone [21, 22]. Following priming and expansion, $CD8^+$ T cells enter an effector phase, trafficking to the red pulp and extravascular sites to eliminate pathogens and infected cells.

During priming, $CD8^+$ T cells and DCs participate in a series of short and long interactions that result in T cell expansion and acquisition of effector functions. It has also been demonstrated that modification of these serial contacts between DC and $CD8^+$ T cells can decrease the tendency to form memory [23]. When studying competition in subsets of $CD8^+$ T cell memory, it is relevant to postulate the role dendritic cells play, whether it is in competition for activation, the target antigen, or signals that can determine memory formation.

What is memory and where is it from?

The classic true-memory $CD8^+$ T cell phenotype can be roughly defined in terms of distinct expression of cell surface makers and the ability to rapidly proliferate and acquire effector functions upon re-exposure to a specific peptide:MHC complexes [24]. The range of cell surface markers include CD44 and CD122 while IL-15 is necessary to maintain the homeostatic turnover of true-memory $CD8^+$ T cells [1]. Again, it is

important to note that this state of true-memory is achieved only after antigen encounter in the context of an immune response.

However, as alluded to earlier, conditions of lymphopenia can occur in hosts, whether it be from chemotherapy, irradiation, viral infections, etc. [25]. During lymphopenia, a phenomenon known as acute homeostatic proliferation occurs; in this process, naïve $CD8^+$ T cells rapidly proliferate and achieve the gene-expression profile and functional status of true-memory cells, without every having been exposed to cognate antigen or endured a classic pathogen-driven immune response [13, 14, 17]. These cells, known as homeostasically proliferating (HP-memory) cells, express the same cell surface markers as true-memory cells (such as CD44, CD122, CD127 and Ly6C) but more importantly, are just as proficient at initiating a rapid and robust response upon exposure to cognate peptide:MHC complexes [13, 14, 16]. It is also relevance that due to the nature in which these HP-memory cells are derived, they have been found to play notable roles ranging from tumor immunology to autoimmunity [25, 26]. It is therefore of interest to discover how well these memory-dopplegangers are able to compete with true-memory T cells, of the same specificity, under conditions of infection.

These concerns are relevant as it has been shown that following subsequent infections with unrelated pathogens, the number of existing antigen-specific T cells are decreased [27]. There is a selective loss of LCMV-specific memory $CD8^+$ T upon infections with heterologous viruses [27]. Additionally, viral infections induce an early event of lymphopenia that results in the attrition of primarily $CD44^{hi}$ $CD8^+$ memory T cells [28]. Therefore, we question whether the response of HP-memory cells will

compromise the activation and expansion of true-memory cells under conditions of competition during infection.

Even as it appears that different states of memory can be achieved outside the context of the classic immune response, there is still no consensus as to the mechanistic transition from a naïve to true-memory $CD8^+$ T cell. It is difficult to characterize which effector cells will transition into memory, primarily because there are no markers that fully differentiate between effector cells destined to survive or die [29]. Ongoing debates in the field posit a range of ideas in programming of memory differentiation being made very early after infection to stochastic mechanisms that divide cells into different states of potential memory cells [30]. In recent years however, it has been revealed that during expansion of naïve T cells, two distinct populations arise with different tendencies to form a long-lived memory population [31]. One population is believed to expand and function as effector cells and is characterized by KLRG-1^{hi} and IL-$7R^{lo}$ expression (termed SLECs, short-lived effector cells), while the other tends to form a stable memory pool and is characterized by KLRG-1^{lo} and IL-$7R^{hi}$ expression (termed MPECs, memory-precursor effector cells) [29, 31]. Of note, most data on this topic has been derived from flow cytometry (FACS); utilizing different methods of analysis can determine the possible anatomic location this phenomenon occurs. It is then of interest to see how the differential expression of markers on SLECs and MPECs correlate to different states of memory and their localization within the secondary lymphoid organs.

Adoptive transfer and infection model

The existence of at least two different forms of memory (true-memory and HP-memory) brings us to question how well HP-memory competes with true-memory cells and whether HP-memory populations compromise reactivation or homeostasis of true-memory cells. With the trends of HP- and true-memory competition, we survey the splenic histology in naïve, HP-, and true-memory immune responses to deduce characteristic localization associated with cells of differing antigen-exposure and states of memory. Finally, we query the trafficking of DCs post-infection with respects to that of naïve, HP-, and true-memory subsets to infer a possible reason for the distinct localization patterns. Unveiling the trends behind memory competition and migration, it would be of value to speculate the functional nature of migration patterns in terms of memory formation. Experiments performed in collaboration with Kitty Cheung.

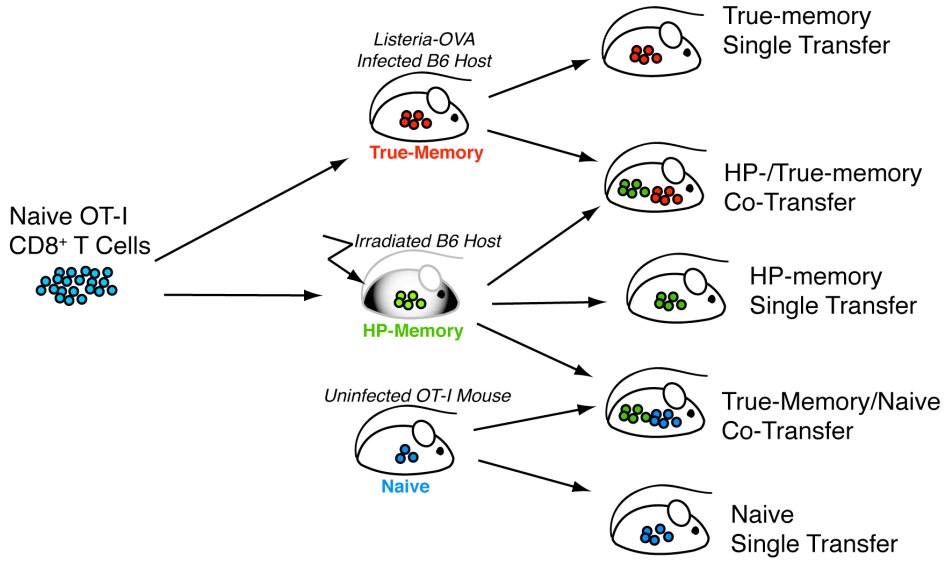

Figure 2: Experimental model
Sources and generation of different memory subsets. To generate HP- or true-memory cells, naïve OT-I CD8$^+$ T cells are transferred into mice either rendered lymphopenic by sublethal irradiation or infected using Listeria-OVA, respectively. To measure the immune response, OT-I CD8+ T cells of different states of memory are then adoptively transferred into B6 mice and subsequently infected using Listeria-OVA. Courtesy of Kitty Cheung.

To examine these aspects about $CD8^+$ T cell memory, we utilized an adoptive transfer system (the transfer of syngeneic cells from one mouse into another) (Fig. 2). Generally, transferred cells were distinguished from those of the host through different congenic markers (CD45.1, CD45.1.2, or Thy1.1) or fluorescence. To investigate the immune response, mice were then challenged using recombinant Listeria-OVA.

In carrying out our studies, we have created true-memory, HP-memory, and naïve cell types from OT-I $CD8^+$ T cells. The use of only OT-I cells, specific for SIINFEKL (OVA-peptide) bound to MHC-I (Fig. 2), ensures a single specificity and equal affinity across all three states of memory. Therefore, this system allows us to study the effects of naïve and different states of memory programming using one antigen specific population of $CD8^+$ T cells. In order to create true-memory cells, we transfer congenically labeled OT-I cells into a C57BL/6 mouse (B6) followed by an infection using Listeria-OVA. After 30 days, transferred OT-I cells attain the true-memory phenotype and are harvested, purified, and transferred into naïve B6 mice to carry out experiments.

To create HP-memory cells, congenically labeled OT-I cells are sorted and transferred into naïve B6 mice that were rendered lymphopenic by sub-lethal irradiation (600rads) 24 hours prior. At least 30 days are allotted for transferred OT-I cells to undergo homeostatic proliferation and become HP-memory. As with true-memory, HP-memory cells are then harvested and purified before transfer into uninfected B6 hosts to carry out experiments.

This system allows us to focus our experiments on the kinetics and response of each memory population. Using single or co-transfers of different memory populations, we are able to study the kinetics and competition amongst these specific memory subsets.

Though flow cytometry provides the means to analyze the kinetics and statistical response of each transferred populations, the trafficking and physical distribution of the different states of memory has yet to be elucidated. The power of histology reveals key patterns in localization that appear to be exclusive to cells that have attained true-memory.

RESULTS

Competition between co-transferred HP- and true-memory CD8$^+$ T cells

True-memory outcompetes HP-memory CD8$^+$ T cells during secondary infection

To study the behavior of the HP- and true-memory cells during infection, three experimental groups (a 1:1 mix of both populations, HP-Memory alone, or true-memory alone) were transferred into new B6 hosts and were infected with Listeria-OVA one day later (Fig. 3A). The co-transfer allowed us to observe how well the HP- and true-memory cells competed for resources and space during infection. The expansion of each subset was monitored by FACS in the peripheral blood (PBL) and spleen. Both subsets responded to infection and underwent significant expansion (Fig. 3B-E). However, in the case of the co-transfer, the true-memory cells displayed increased expansion and formed more secondary memory than the HP-memory cells, despite the HP-memory undergoing earlier expansion (Fig. 3B). This early accumulation did not persist and the HP-memory cells ultimately generated fewer secondary memory cells. Similar results were observed during i.v. infection with Vesicular Stomatitus virus expressing OVA and when using P14 transgenic HP-memory CD8$^+$ T cells responding to lymphocytic choriomeningitis virus administered i.p. (data not shown). Thus, the inability of HP-Memory to compete with true-memory was not pathogen, route or TCR specific.

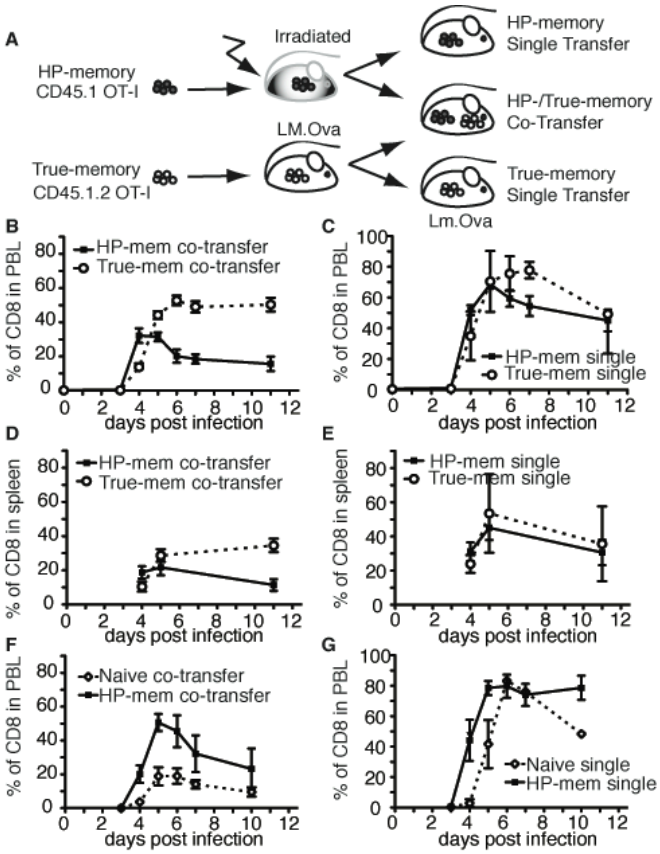

Figure 3: True-memory CD8$^+$ cells outcompete HP-memory cells during secondary infection. **(A)** Generation of memory T cell subsets and experimental design. Immune response of the donor memory subsets was measured as a percentage of the total CD8$^+$ cells in the indicated tissue. **(B)** Co-transfer: HP- and true-memory, PBL. **(C)** Single transfer: HP- and true-memory, PBL. **(D)** Co-transfer: HP- and true-memory, spleen. **(E)** Single transfer: HP- and true-memory, spleen. **(F)** Co-transfer: naïve OT-I and HP-memory, PBL. **(G)** Single transfer: naïve OT-I and HP-memory, PBL. Courtesy of Kitty P. Cheung.

In the absence of a competing memory subset, the HP-memory response largely mirrored that of the true-memory, accumulating to similar levels and forming equivalent amounts of secondary memory in the PBL (Fig. 3C, E). There were minor differences in the contraction phase, where the HP-memory peaked earlier than the true-memory cells; however they consistently formed robust "secondary" memory. The differences observed in the PBL between the single and competing memory cell transfers were reflected in the splenic analysis (Fig. 3D, E).

These results raised the possibility that the HP-memory $CD8^+$ T cells were not able to compete well with true-memory cells in spite of their ability to expand, protect, and form secondary memory when they act as the sole antigen-specific population. To assess the ability of the HP-memory cells to compete with other T cell subsets, we next compared their ability to compete with naïve cells bearing the same TCR specificity after infection (Fig. 3F). Compared with the naïve OT-I cells in the co-transfer, the HP-memory cells expanded first and to a greater degree, and formed more secondary memory, correlating with the single transfer kinetics (Fig. 3G). Thus, the HP-memory out-compete naïve cells of the same specificity by providing more rapid expansion, greater secondary memory formation (Fig. 3F, G), and enhanced protection [32].

Taken together, these data suggest that during infection, HP-memory cells are at a disadvantage when competing with their true-memory counterparts for limited resources, despite their ability to out-compete naïve T cells. Upon infection, significant HP-memory cells traffic to the lymph nodes, but pooling both spleen and lymph node HP-memory cells still does not make up for the deficit (data not shown). Thus, we find that while the HP-memory population is phenotypically and functionally similar to true-memory, it is not an exact substitute.

HP- and true-memory cells display distinct localization patterns within the spleen

We next examined HP- and true-memory $CD8^+$ T cell localization within the spleen during infection with Listeria-OVA. The differential expansion of HP- and true-memory cells seen by FACS poses the question of whether localization patterns of either subset indicate exclusive access to stimulatory signals. Early post-infection (Days 1-2),

we found that HP- and true-memory cells both localize to the periarteriolar lymphoid sheath (PALS), also known as the T cell zone (Fig. 4).

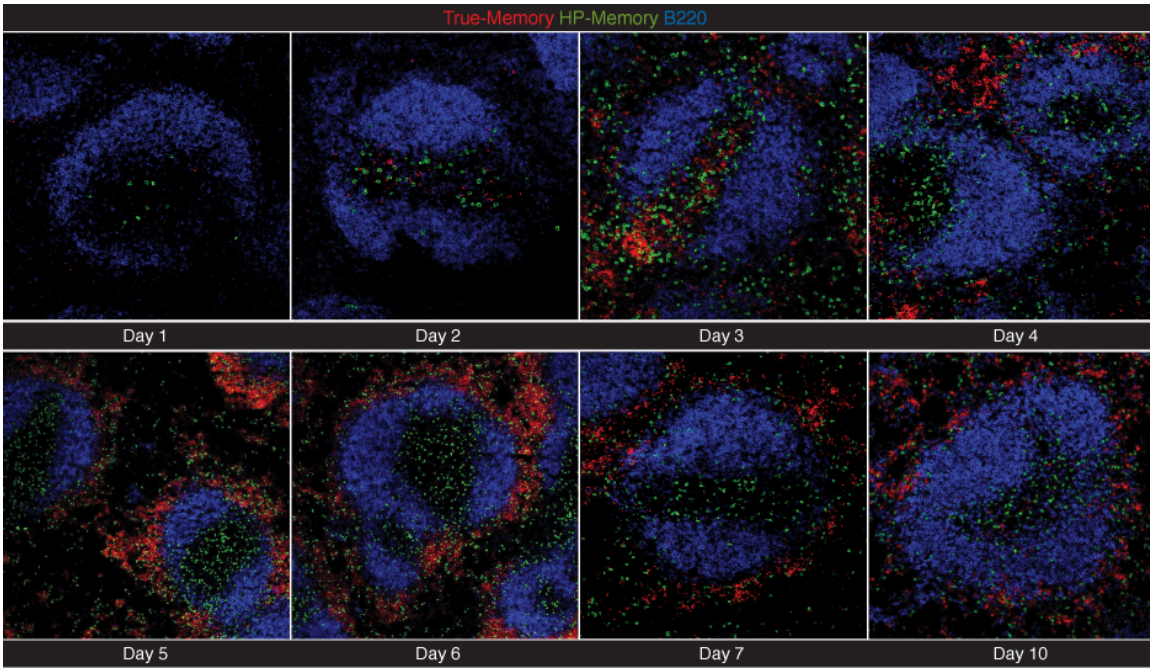

Figure 4: Timecourse of HP- and true-memory cell localization following co-transfer.
HP- and True-memory were co-transferred into B6 hosts and infected with Listeria-OVA. Localization of respective donor cells in the spleen on days 1-10 after infection was evaluated by staining for congenic markers CD45.1 (HP-Memory) , Thy1.1 (True-Memory), and B220. (B cells).

This indicated that the HP-memory cells were initially located appropriately for antigen recognition, consistent with the fact that HP-memory did not show a defect in expansion during the first four days of infection (Fig. 3). However, starting day 4 and evident by day 5, true-memory cells had localized to the marginal zone (MZ) and red pulp (RP) (Fig. 4). In contrast, a significant population of HP-memory cells remained in the PALS.

This striking difference between HP- and true-memory cell localization within the spleen was accentuated as the infection progressed. Higher magnification images of the mid and late timepoints, when the phenotype is most drastic, better portray the distinct localization patterns seen in HP- and true-memory cells (Fig. 5).

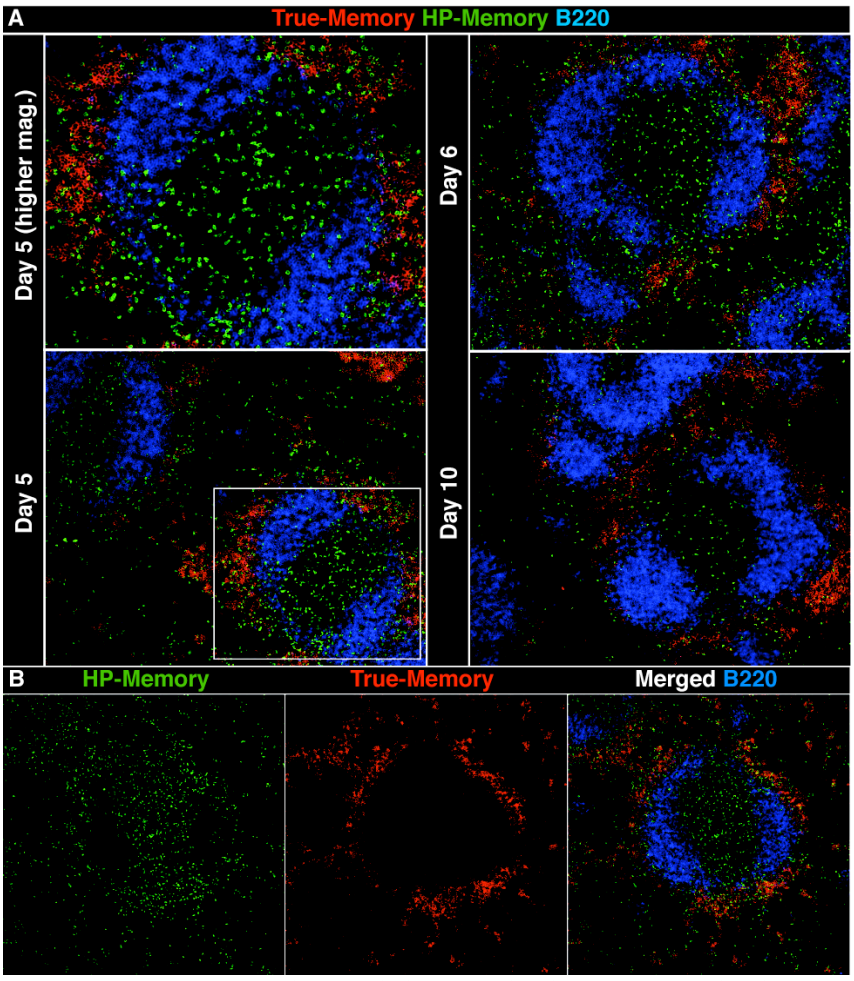

Figure 5: HP- and true-memory cells display distinct localization and clustering in the spleen. HP- and True-memory were co-transferred into B6 hosts and infected with Listeria-OVA. **(A)** Spleen sections of co-transfer recipients on timepoints with most drastic localization – days 5, 6 and 10. Stained for both memory subsets and B220. **(B)** Individual panels with the indicated stains and merged image of spleen (Day 5).

By day 5 of infection, the true-memory cells were already largely absent from the PALS and accumulated in the RP/MZ along the edge of the B cell follicle (Fig. 5A). In contrast, the HP-memory cells were still abundant in the PALS and were also scattered throughout the RP and even regions of the B cell zone. Analyzing single color channels even on day 5 post-infection, the drastic difference in localization is clear, as HP-memory cells were rarely found in clusters and only a portion co-localized with the true-memory cells along the B cell follicle edge (Fig. 5B). On day 10 post-infection, significant

numbers of HP-memory cells remained in the PALS while true-memory cells were observed mainly in the RP/MZ regions (Fig. 5A). The localization of true-memory cells to the RP/MZ under conditions of competition suggests that they possess an advantage over HP-memory cells in accessing certain signals localized in the RP/MZ.

Splenic localization of single transfers of HP- and true-memory cells

Co-transferred HP- and true-memory $CD8^+$ T cells display distinct localization patterns; we then observed the localization of HP- and true-memory single transfers to determine if the presence of true-memory cells altered the ability of HP-memory cells to access the RP/MZ under conditions of competition. Though notable single-transferred HP-memory cells still remain in the PALS following an infection by Listeria-OVA, we find that they now display an intermediate phenotype compared to HP-memory cells competing with true-memory cells (Fig. 6). This intermediate phenotype is defined by significantly greater cell numbers in the RP/MZ, and correlates with single HP-memory immune responses evidenced by FACS (Fig. 3E) – single transferred HP-memory cells expand to similar levels as true-memory cells and form the same amount of secondary memory. In short, the general localization patterns seen in single transferred HP-memory cells suggests that when not competing against true-memory cells, HP-memory cells appear more capable of accessing the RP/MZ.

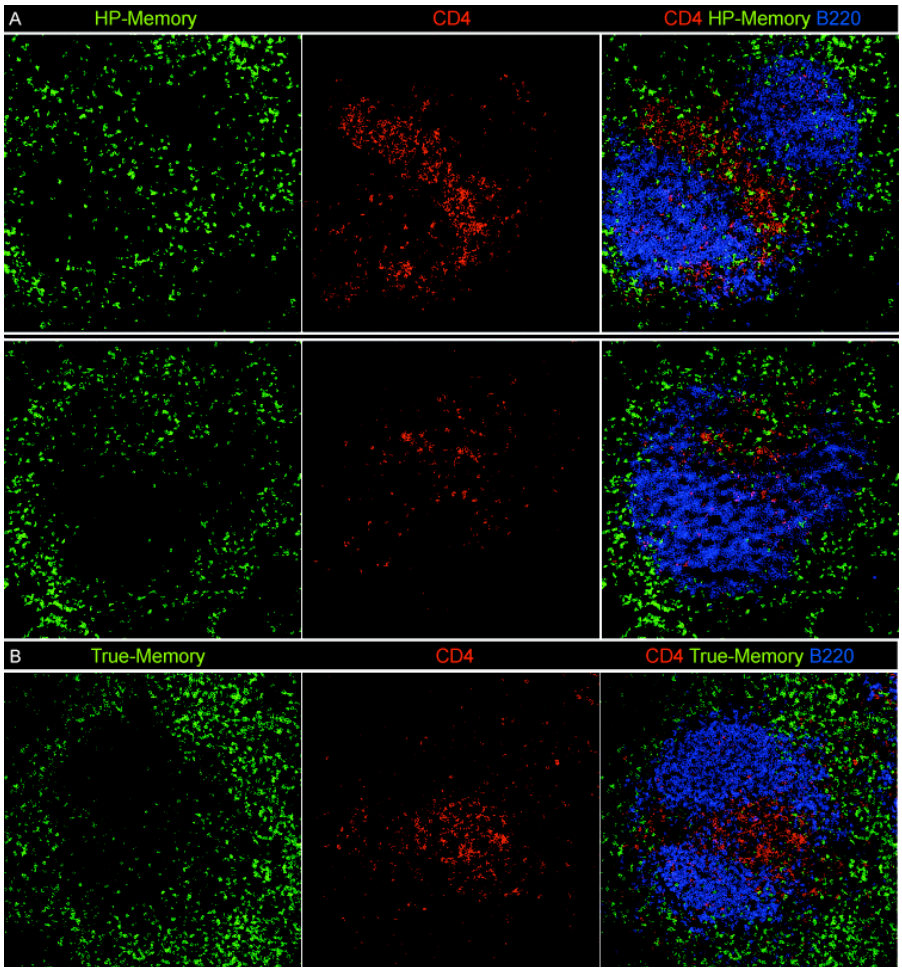

Figure 6: Localization of single transfers of HP- or true-memory cells. HP- or true-memory cells were single transferred into separate B6 hosts and challenged with Listeria-OVA. Images depicting the localization of **(**A) HP-memory and (B) true-memory cells.

Differential mRNA expression for chemokine receptors by HP-memory cells

The differential trafficking by the HP-memory cells led us to investigate chemokine receptor expression by the two memory subsets using a chemokine/chemokine receptor qPCR array. On day 6 of infection, when there was clearly significant differences between the localization of the subsets, HP- and true-memory cells were sorted from pooled spleens of co-transfer recipients. Relative mRNA levels for 84 genes, comprised primarily of chemokines and chemokine receptors, were

evaluated by qPCR. Figure 7 summarizes the target genes that have 2-fold or greater difference in expression between HP- and true-memory cells.

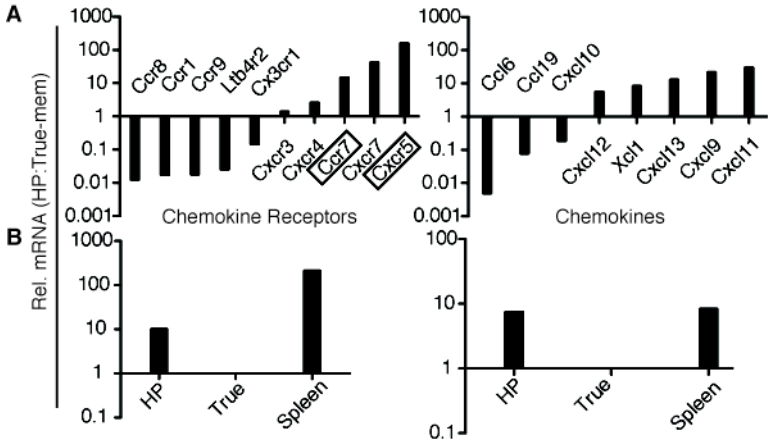

Figure 7: mRNA levels of chemokines and chemokine receptors by HP- and true-memory cells. cDNA was generated from co-transferred HP- and True-Memory cells sorted from pooled spleen (Day 6). Relative mRNA levels for indicated genes were determined with a qPCR array and normalized to GAPDH. **(A)** The transcripts displaying a 2-fold or greater difference in expression were listed and further divided into receptors (left) and chemokines (right). **(B)** qPCR verification of CXCR5 and CCR7 mRNA levels. mRNA from total spleen used as a reference. Courtesy of Kitty P. Cheung.

Of particular interest were the chemokine receptors CXCR4, CXCR5, CXCR7, and CCR7, which have roles in lymphocyte homing in secondary lymphoid organs (Fig. 7). HP-memory cells expressed ~10-fold more CXCR5 mRNA than the true-memory controls (Fig. 7A, B left). While the function of CXCR5 on $CD8^+$ T cells is not well characterized, CXCR5 expression on $CD4^+$ T helper cells mediates their localization to the B cell follicle [33]. CXCR4 and CXCR7 both bind to CXCL12, a chemokine found in the B cell zone, but are not characteristically expressed by $CD8^+$ T cells [3]. CCR7 was also upregulated on HP-memory cells (Fig 7A, B right) and mediates T cell and dendritic cell (DC) homing and positioning in the T cell zone. CCR7 ligands are known to be secreted by DC, macrophages, and stromal cells in the T cell zone [3]. Increased expression of CCR7 and chemokine receptors that mediate homing to the B cell follicle

may explain why a significant portion of the HP-memory cells were retained in the PALS and B cell zone and why they displayed disorganized localization compared to the true memory cells.

Co-transferred HP- and true-memory dendritic cell studies

As mentioned earlier, dendritic cells (DCs) play indispensable roles in activating and inducing memory formation in $CD8^+$ T cells [21]. These signals include MHC:peptide interactions, co-stimulation through the B7 molecule, or cytokines. The ability of a $CD8^+$ T cell to access DCs can determine the degree of activation and proliferation. It therefore possible that DCs provide the sources of RP/MZ signals for both memory subsets. We explored the localization patterns of DCs to determine if co-transferred true-memory cells possess an advantage over HP-memory cells in accessing DCs.

To detect the presence of dendritic cells, we stained for CD11c, a marker primarily found on DCs. Shown earlier, co-transferred HP- and true-memory cells expand to similar levels early in the immune response, but true-memory cells out-compete HP-memory cells by the mid and late timepoints (Fig. 3E).

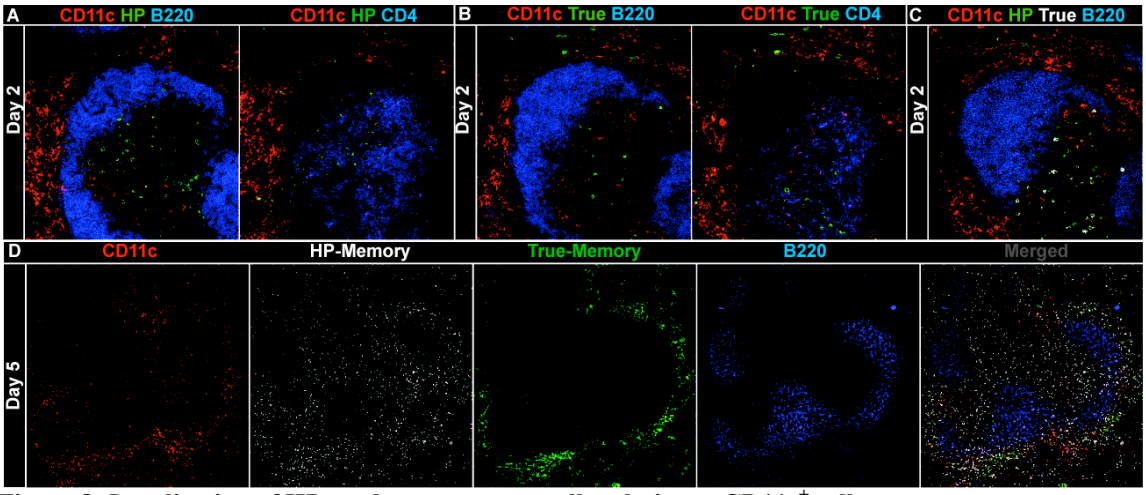

Figure 8: Localization of HP- and true-memory cells relative to CD11c$^+$ cells.
Confocal images of serial spleen sections from co-transfer recipients. (Day 2 of infection). Sections were stained for CD11c, B220 or CD4, and congenic markers for: **(A)** HP-memory, **(B)** True-memory, **(C)** HP- and true-memory. **(D)** Spleen (Day 5) was stained for CD11c, both memory subsets, and B220.

Using a co-transfer scenario of HP-memory versus true-memory, CD11c staining was correlated to timepoints on which the localization patterns of the two memory subsets were both similar (early) and different (mid-late) (Fig. 8). As early as day 2 post-infection, HP-memory and true-memory cells could be seen congregating in particular PALS. Serial sections stained for either HP-memory, true-memory, or both showed that both memory subsets traffic to the PALS early on in order to commence clonal selection and expansion (Fig. 8A, B, C).

CD11c, true-memory, and HP-memory staining within the PALS at early timepoints suggested also that both memory subsets were exposed to proper signals and have similar access to antigen-peptides. However, the intensity of CD11c staining surrounding the white pulp indicated significant populations of dendritic cells were present; CD11c staining of uninfected spleen sections suggest they may be splenic dendritic cells surrounding the white pulp (data not shown). It was not until approximately day 5 that true-memory cells showed their distinct localization to the

RP/MZ while HP-memory cells appeared to be allocated almost equally between red pulp and PALS (Fig. 8D). Looking at CD11c, it appeared that there is still stronger and more significant staining of CD11c in the RP/MZ. This finding suggested a possibility that true-memory cells may interact more with dendritic cells in the later phases of the immune response, acquiring signals that attribute to increased expansion and survival. Alternatively, the antigen-experienced programming of true-memory cells may also allow those effector cells greater access to antigenic and cytokine signals localized to the RP/MZ.

Comparative localization studies of single transferred naïve and true-memory cells

Comparison of naïve and true-memory responses to infection

The trends in localization and kinetics revealed in HP- and true-memory experiments led us to investigate these parameters in single-transferred naïve and true-memory immune responses. Naïve and HP-memory $CD8^+$ T cells share the key trait of never having seen antigen, and we asked whether the migration patterns of single transferred naïve $CD8^+$ T cells reveal any overlapping characteristics with HP-memory localization. Utilizing the adoptive transfer system described above, we individually transferred $8x10^4$ naïve or true-memory $CD45.1^+$ OT-I cells into B6 hosts; each mouse was then infected i.v. with $5x10^3$ Listeria-OVA. The kinetics of the immune response are shown for the percentage of OT-I $CD8^+$ T cells in peripheral blood (PBL); as expected, true-memory cells responded quickly and robustly while naïve cells were delayed in

clonal selection and expansion (Fig. 9). By day 10 post-infection, true-memory cells contracted less than naïve cells and began to differentiate into secondary memory.

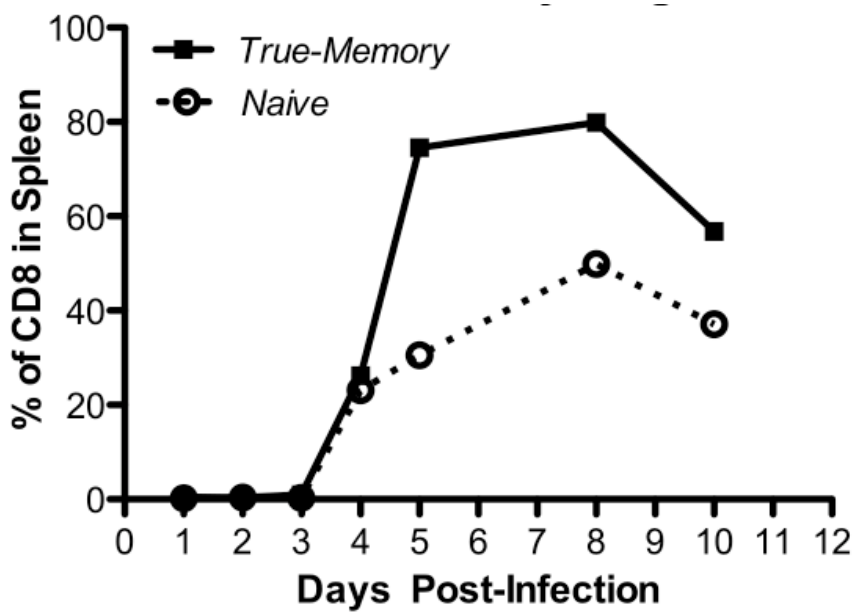

Figure 9: Naïve and true-memory immune response against infection.
$8x10^4$ naïve or true-memory OT-I $CD8^+$ T cells were single transferred into separate B6 hosts and subsequently infected using Listeria-OVA. Immune response of the donor subsets was measured as a percentage of the total $CD8^+$ cells in the spleen.

Localization of single-transferred Naïve and true-memory cells during infection

Next, we transferred either naïve or true-memory cells into separate B6 hosts followed by infections using Listeria-OVA. Immunofluorescence staining was performed on days 1-5, 8, and 10 of single transferred naïve or true-memory splenic tissue sections. To denote splenic architecture, staining with CD4 highlights the PALS while B220 marks the B cell zone. In the early timepoints post-infection, naïve cells are found almost exclusively in the PALS (Fig. 10).

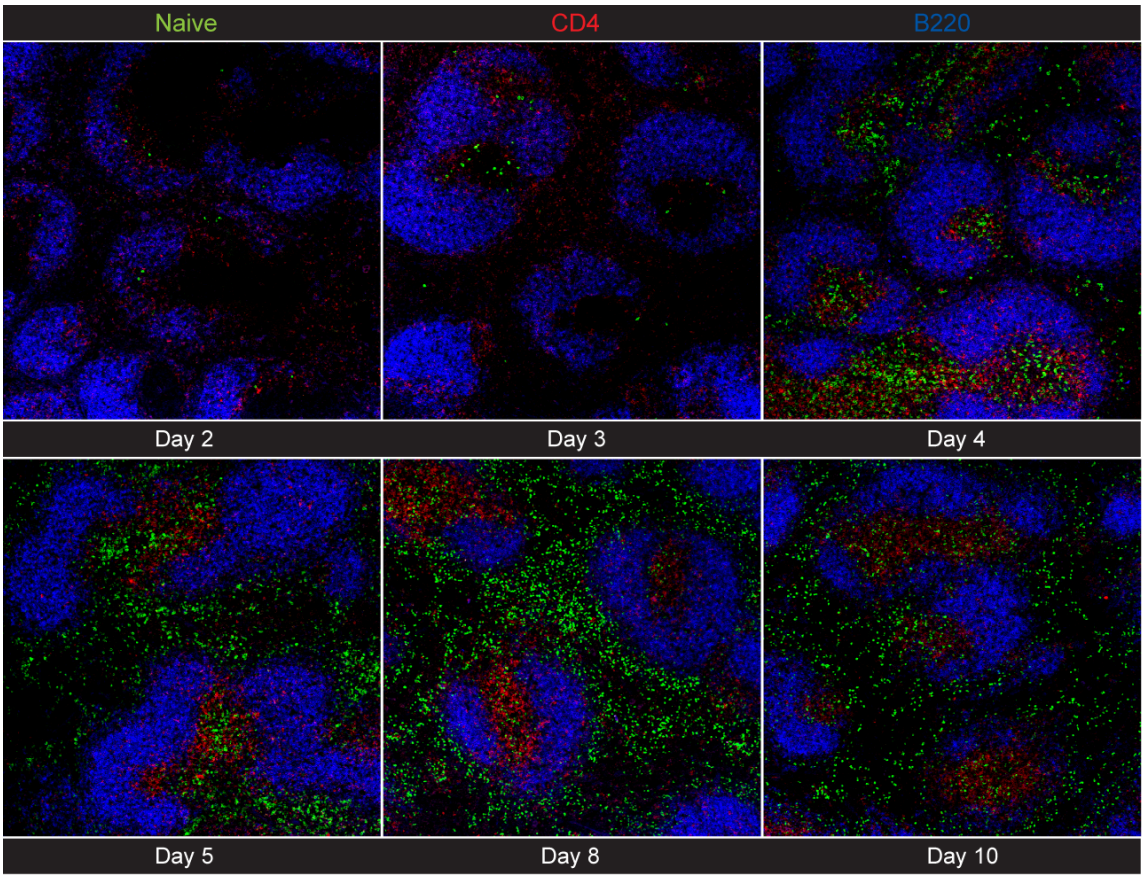

Figure 10: Timecourse of localization of naïve immune response.
Naïve OT-I cells were transferred into B6 hosts and infected with Listeria-OVA. Confocal images of localization kinetics within spleens of naïve cells are displayed for days 2-10. Staining for CD4 (red), B220 (blue), and CD45.1 (green, Naïve).

On day 2 of infection, a few of the naïve cells can be seen within the splenic PALS; on day 3, appear to begin to undergoing clonal expansion. By day 4, a large population of proliferated naïve cells is present in the PALS, while some appear to be moving into the red pulp. At day 5 post-infection, a sizable number of naïve cells that have migrated to the red pulp, possibly to exit into the bloodstream as $CD8^+$ effector cells and traffic to extravascular sites, but clusters of cells still exist in the PALS. Even in the later phases of the naive immune response, the splenic localization patterns appear similar to the mid phases (day 5), except with increased number of naïve cells in the RP/MZ. By day 10,

there still remains a significant population of naïve cells in the PALS as the number of OT-I cells in the RP/MZ begins to wane.

In contrast, the true-memory response presented a distinctly different localization pattern. Even though both naïve and true-memory subsets appear to traffic to the PALS early (day 2), there is already significant proliferation occurring in several true-memory PALS, as would be expected due to the faster kinetics of memory cells (Fig. 11). By day 4, however, large populations of true-memory cells can already be seen exiting the PALS and residing in clusters in the splenic red pulp. Compared to matched naïve timepoints,

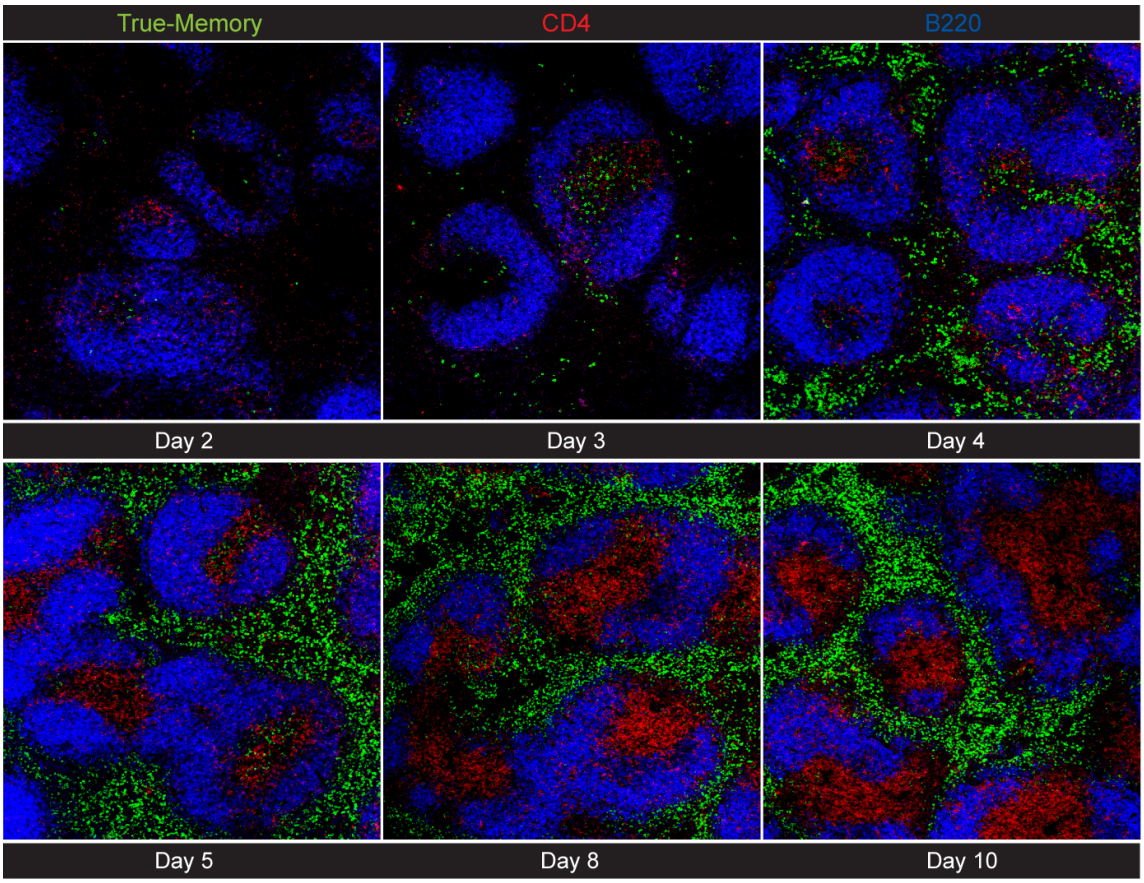

Figure 11: Timecourse of localization of true-memory immune response.
True-memory OT-I cells were transferred into B6 hosts and infected with Listeria-OVA. Confocal images of localization kinetics within spleens of true-memory cells are displayed for days 2-10. Staining for CD4 (red), B220 (blue), and CD45.1 (green, naïve).

many true-memory PALS by day 5 are already nearly void of antigen-specific true-memory cells while the red pulp was filled with clusters of true-memory cells. The difference in localization becomes most apparent and complete by days 8 and 10, as very few to no true-memory cells can be found in the PALS when compared to late timepoints in the naïve response; the majority of true-memory cells on day 10 reside in clusters that fill the splenic red pulp.

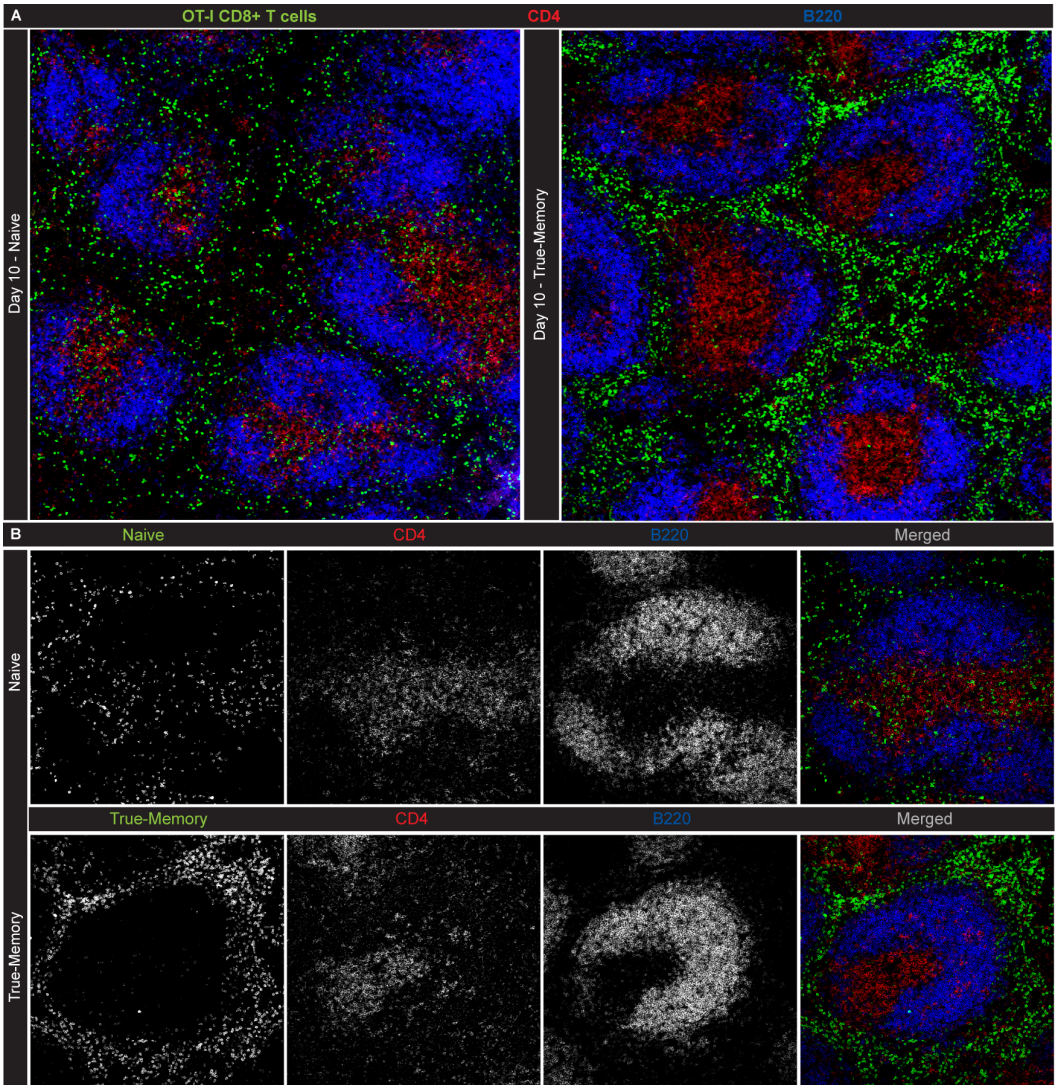

Figure 12: Naïve and true-memory cells also display distinct localization patterns within the spleen. Comparison of localization patterns in single transfers of naïve or true-memory cells upon post-infection using Listeria-OVA. **(A)** Overall 10X magnification comparison of naïve and true-memory localization in splenic sections on day 10 post-infection. **(B)** Comparison of 20X magnification images of single naïve or true-memory white pulps.

Since the differential localization between naïve and true-memory subsets is most apparent on day 10, we took a closer look by comparing higher magnification images of single white pulps for both subsets (Fig. 12B). As seen in the spleen, naïve T cells in the late day 10 timepoint are distributed nearly equally amongst the PALS and red pulp, leaving a significant population of these antigen specific cells in the PALS (Fig. 12A). The true-memory spleen reveals a nearly opposite pattern – very few antigen specific cells are present in the PALS while highly dense clusters of those clones populate the red pulp. When comparing higher magnification raw, uncolored single-stain images of individual white pulps, the differential localization patterns of naïve and true-memory OT-I cells becomes more apparent (Fig. 12B). Few true-memory cells remain within the PALS, delineated by CD4 staining, while large numbers of naïve cells prevail, co-localizing with CD4 T cells.

Taken together, there appears to be a distinct localization phenotype also associated with antigen-experienced cells that have been fully programmed into true-memory cells. The classic robust memory immune response typically displayed by FACS is reflected in the splenic histology by sheer number of antigen-specific cells present. However, what histology reveals is that true-memory responses almost completely lack a significant population of $CD8^+$ T cells in the PALS. This finding reveals the possibility that there may be signals within the PALS necessary for naïve $CD8^+$ T cells to be programmed into antigen-experienced true-memory and attain its functional characteristics. As alluded to in the experiments demonstrating DC localization in co-transferred HP- and true-memory cells (Fig. 9), there could be signals accessible only by true-memory cells in the RP/MZ due to their antigen-experienced memory programming.

An apparent key difference between true-memory and naïve cells is the acquisition of the memory-state following antigen encounter. The differential localization patterns between naïve and true-memory cells may elucidate this phenomenon through the possibility that signals within the PALS influence memory formation.

Naïve and true-memory dendritic cell studies

We looked more closely at the DC localization within single transfers of naïve or true-memory OT-I cells followed by intravenous infections using Listeria-OVA. Again, we find that staining patterns for CD11c change throughout the infection, but naïve and true-memory localization patterns are still reflective of previous experiments (Fig. 13). In the following experiments, "early" timepoints are defined roughly as days 1-3 (day 2 shown), "middle" timepoints as days 4-6 (day 5 shown), and "late" timespoints as days 7-10 (day 10 shown).

At early timepoints, CD11c staining is strong and appears in tight rings around each splenic white pulp and in most PALS, fitting with the timing at which clonal selection and expansion of antigen-specific T cells is occurring (Fig. 13).

Figure 13: Localization of single-transferred naïve and true-memory cells relative to CD11c+ cells within the spleen.
Single transfers of naïve and true-memory cells into B6 hosts subsequently infected using Listeria-OVA. Single stain and merged images of splenic sections are shown to display the kinetics of CD11c relative to **(A)** naïve or **(B)** true-memory cells. Days 2, 5, and 10 shown are representative of the "early", "mid" and "late" phases of the immune response. Sections are stained for CD11c (red), CD45.1 (green, respective memory sub-sets), and B220 (blue).

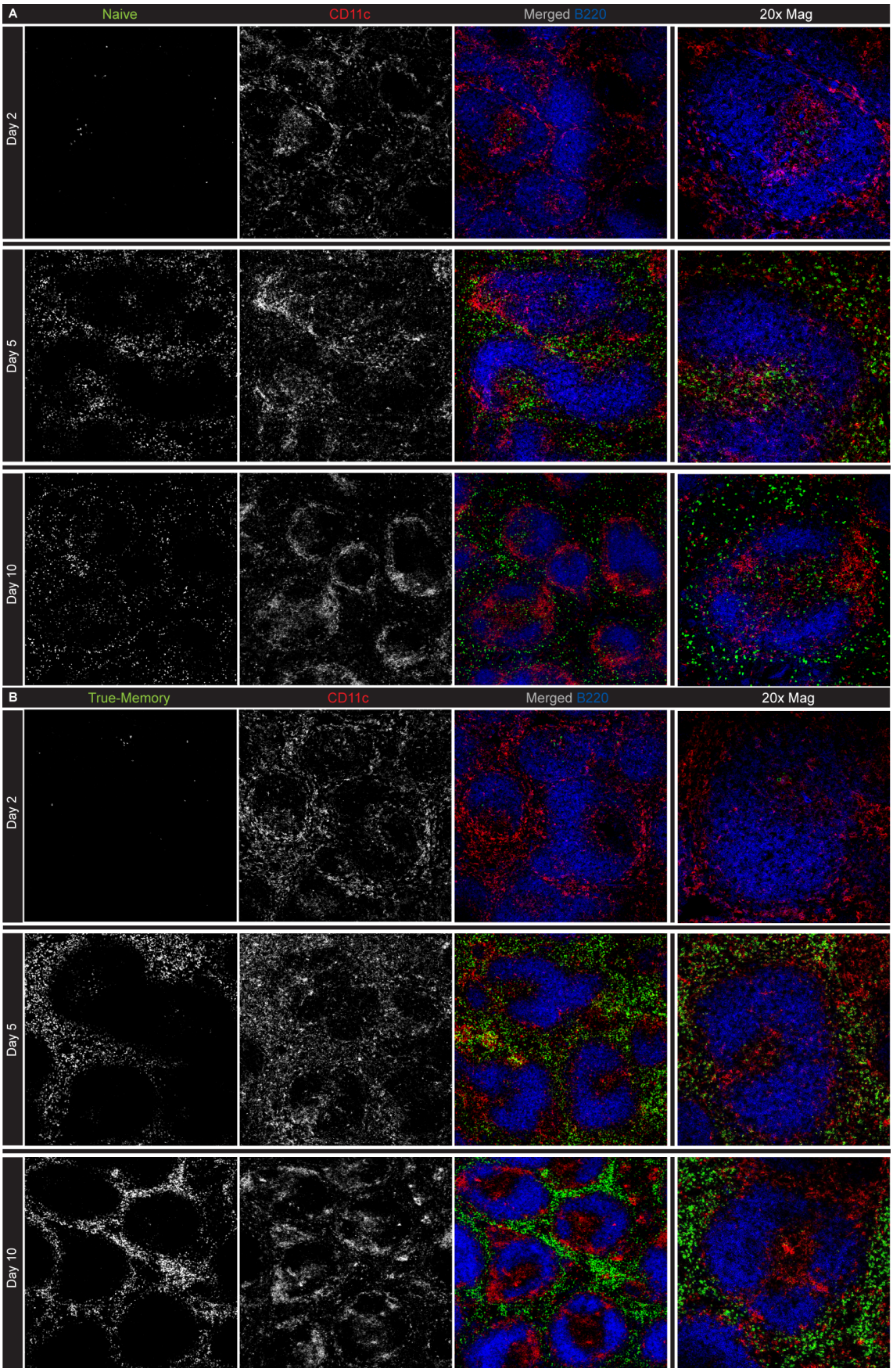
A
Naive
CD11c
Merged B220
20x Mag
Day 2
Day 5
Day 10
B
True-Memory
CD11c
Merged B220
20x Mag
Day 2
Day 5
Day 10

By the mid-point of infection, this pattern of CD11c staining begins to change, becoming widespread and scattered, appearing in most PALS and filling the RP/MZ in both naïve and true-memory transferred hosts. It is also important to note that there are other cell types within the spleen that upregulate the CD11c marker under conditions of infection and inflammation [34], thus these cells are referred to as $CD11c^{+}$ cells rather than dendritic cells. However, the CD11c staining changes again in the later phase of the immune response; in both hosts, the marker appears to form intensely staining clusters that fill the PALS and encircle portions of the white pulp.

Recalling that a significant number of naïve cells still populate the PALS by day 10, the intense staining of CD11c clusters within the PALS suggests that there may be signals and resources in the region that are necessary for non-antigen-experienced cells to attain the state of true-memory. Conversely, the bright staining of CD11c surrounding the white pulp at late timepoints could also indicate that there are signals in the RP/MZ that promote the accumulation of secondary true-memory, inaccessible to non-antigen-experienced cells. Vast numbers of true-memory cells fill the red pulp with little to no true-memory OT-I T cells found within the PALS (Fig. 13B). Taken together with the late phase CD11c staining, these patterns of naïve and true-memory localization fit with a key difference between true-memory and other antigen-inexperienced subsets – that true-memory cells have already undergone the full process of memory programming.

DISCUSSION

Uncovering the signals and cell-cell interactions responsible for generating immunological memory is a task that must be approached from multiple angles. We questioned the role that competition plays among memory $CD8^+$ T cells of the same specificity, as it has been demonstrated that attrition of memory T cells occurs in subsequent heterologous infections [27, 28]. The trends in memory T cell competition led us to investigate peculiarities in splenic localization patterns through the timecourse of the immune response and the possible function of DCs in the processes of selective priming and memory formation. Our studies have unveiled a few more pieces of the puzzle through histological analyses of the immune response in different states of $CD8^+$ T cell memory.

In our experimental setup, we adoptively transferred congenically labeled OT-I $CD8^+$ T cells (one specificity) of naïve or different memory states (HP-/ true-memory) into B6 hosts, followed by infection using Listeria-OVA to generate a secondary immune response (Fig. 2). In short, this system utilizes the advantage of limiting our $CD8^+$ T cell specificities to a single transgenic population, allowing us to study the variance of different states of memory expressing the same antigen specificity.

In the competition between the HP-memory and true-memory OT-I cells, we find that true-memory cells always prevail upon antigenic challenge, whether it is in overall expansion or formation of secondary memory (Fig. 3). This is in contrast to single transfers of these subsets into B6 hosts followed by infection – the HP-memory expansion is similar to that of true-memory, and HP-memory cells form the same level of

secondary memory (Fig. 3). Previous experiments found that HP-memory cells shared a similar gene-expression profile with that of true-memory [15] and possess true-memory functional characteristics [13, 14, 16]. Thus, it was surprising that HP-memory cells deferred so substantially to true-memory cells when competing during an infection.

However, despite the acquisition of a memory-like phenotype by HP-memory cells, signals promoting HP- and true-memory cell differentiation are quite distinct. The initial naïve $CD8^+$ T cell response to infection and subsequent formation of a memory population requires TCR-mediated recognition of pathogen-derived peptide/MHC class I complexes on professional antigen-presenting cells, co-stimulatory signals and inflammatory cytokines [1]. In contrast, acquisition of a memory phenotype by naïve cells during lymphopenia-induced proliferation is triggered by low-affinity interactions with self-peptide/MHC complexes and IL-7 [12, 13] and is co-stimulation independent [14, 35]. As mentioned, previous experiments demonstrate that HP-memory cells can essentially mirror the functional characteristics of true-memory, but there are still key differences in their formation, namely the process of memory programming induced through antigen experience.

In light of the kinetics during competition (Fig. 3), we utilized histology to explore the spleen for aberrant localization patterns. In short, both subsets localized to the PALS in the early expansion phase, indicating equal access for antigen presentation and activation signals [36], but true-memory cells in the mid- and late-phases of the immune response traffic primarily to the RP/MZ, accumulating in dense clusters and leaving little to none in the PALS (Fig. 4, 5). Significant populations of naïve and HP-memory cells remain within the PALS throughout the timecourse (Fig. 4, 5). This may indicate that

true-memory cells hold an advantage in obtaining signals from the RP/MZ. T cell trafficking between the PALS and B cell zone has been shown to be dependent on ratios of CCR7 and CXCR5 expression [37]. Performing an assay for chemokine and chemokine receptor mRNA expression, we find also that HP-memory cells display ~10-fold greater expression of CCR7 and CXCR5, which may partially explain why they remain within the PALS (Fig. 6). Even given this possible mechanism, such an anomaly in HP-memory localization patterns combined with the competitive hierarchy revealed by FACS poses a question as to why, functionally, there remains a population within the PALS in HP-memory but not true-memory.

Before exploring the possible reasons for differential trafficking in $CD8^+$ memory subsets, it is important to include in this discussion the migration patterns of single-transferred naïve cells (Fig. 11, 13). The kinetics of a single transfer of true-memory OT-I cells into subsequently infected B6 hosts show, as expected, localization patterns that mirror those observed in HP-memory and true-memory co-transfers – cells in the late phase are nearly absent from PALS, but cluster to fill the RP/MZ (Fig. 12, 13). Surprisingly, the naïve response reveals trafficking patterns that appear nearly identical to that of HP-memory, with significant populations of effector cells derived from naïve cells situated within the PALS during the late phase (Fig. 7, 11, 13). These similarities in localization are further highlighted when comparing HP-memory single transfer images (Fig. 7) with those of naïve cells (Fig. 11, 13). Taken together, the strikingly similar trends in localization between naïve and HP-memory cells reveal another possible basis as to why such $CD8^+$ T cell from non-antigen-experienced populations exist in the PALS

– that neither has been exposed to antigen. It is this key trait that may explain the similar trafficking pattern seen in both naïve and HP-memory cells.

True-memory cells possess the ability to re-activate rapidly and undergo robust expansion [1]. Unexpectedly, HP-memory cells can also attain these characteristic true-memory functions, but through acute proliferation during conditions of lymphopenia [12]. However, even though they can arguably substitute for true-memory, it is still not certain if these cells are fully programmed into antigen-experienced true-memory cells. The failure of HP-memory to compete well against true-memory cells and the similarities to naive localization patterns may suggest the latter. Since the PALS (the T cell zone) is often thought of as the site of T cell activation, there may be certain signals within this region that are necessary to unlock the abilities of the true-memory phenotype in naïve cells, or more broadly, cells that have never been exposed to antigen. This idea coincides with the observation that true-memory cells rapidly migrate towards the RP/MZ shortly after activation [22]. Furthermore, it is also known that naïve $CD8^+$ T cells must undergo a series of short serial and long duration interactions with antigen-containing DCs in order to initiate an effector response as well as proper memory formation [23, 38]. Seeing as how secondary (post-response) HP-memory cells do outcompete primary true-memory cells (data not shown), there may be a crucial signal that is only received within the PALS. The possible functional aspect of these signals can vary – the signal may be important in inducing memory programming. Alternatively, acquisition of signals previously may allow responding cells to access any stimulatory signals or cytokines in the RP/MZ upon future antigenic encounter. The localization of true-memory cells to the RP/MZ may suggest that they are no longer reliant on certain signals within the PALS.

These speculations bring about the hypothesis that the PALS is the site which seeds the memory compartment.

To address the notion of localization being dictated by the PALS, we decided to explore any peculiarities with DC kinetics. Mentioned above, DCs influence the level or duration of antigen exposure [23, 38] as well as co-stimulation and cytokine availability, which dictates expansion and memory formation [3]. Staining for $CD11c^+$ cells along with HP-/true-memory co-transfers (Fig. 9) or naïve/true-memory single-transfers (Fig. 14), we find that there are no notable differences in the early expansion phase of the immune response – all memory subsets are localized to the PALS, where there is evident $CD11c^+$ staining. When analyzing mid-phase timepoints of HP- and true-memory co-transfers, it appeared as if $CD11c^+$ staining appeared stronger in the RP/MZ, suggesting that DCs may carry some signal that is accessible only by co-localized cells (Fig. 9D). However, closer analysis of naïve and true-memory timecourses reveal a reshaping pattern of CD11c staining throughout the phases of infection (Fig. 14). As previously shown, $CD11c^+$ staining by the mid-phases of infection appear diffuse, but during the later phases concentrate into distinctly dense and strong staining rings that encircle the white pulp and populate the PALS (Fig. 14). Though this intriguing pattern does appear to suggest some sort of process occurring either within the PALS or directly in the RP, this pattern is ultimately inconclusive as there are two issues: 1) whether all $CD11c^+$ cells are DCs and 2) the identity of those cells presenting actual cognate antigen.

It is documented that in an uninfected spleen, the vast majority of $CD11c^+$ cells are DCs, but upon infection, this profile can rapidly shift as many other mononucleated cell types will upregulate the marker [34]. In addition, not all APCs within the spleen will

be presenting the antigen of interest. To address these two issues simultaneously, we initially used an antibody specific to SIINFEKL (OVA-peptide) bound to MHC-I, the molecule recognized by the OT-I $CD8^+$ T cell. However, the tremendous background and low binding affinity of the antibody produced inconclusive results. We next utilized bone-marrow derived, fluorescently labeled, peptide-pulsed DCs, as these DC immunizations are known to be sufficient in inducing an immune response [39]. A definite immune response was achieved, as all OT-I memory subsets expanded, but DCs were undetectable in splenic sections at any timepoint, leaving the anatomical localization of antigen presentation still unknown (data not shown). Though DCs were injected intravenously via the tail vein into mice, it is possible that the target cells migrated to other sites in the path of circulation, namely the lungs and liver [40].

To tackle the issue of deducing which APCs are displaying the target antigen, it is likely that future direction will employ the power of T cell receptor tetramers [41]. Similar to well-known MHC tetramers, T cell tetramers are essentially soluble T cell receptors arranged into a complex of four molecules [42], increasing binding affinity and specificity dramatically over antibodies of similar function. Functioning as actual T cell receptors, these complexes are capable of pinpointing any cell that expresses the specific antigen peptide bound to MHC [41]. Therefore, this system will allow detection of antigen carrying DCs throughout the course of an actual *in vivo* infection using Listeria-OVA. However, the most difficult obstacle in this route is that these molecules are not commercially available, as they have proven to be extremely laborious in design and production [41, 43].

Though the localization of antigen-loaded DCs is unclear, we have shown that populations of non-antigen-experienced (naïve/ HP-memory) $CD8^+$ T cells remain within the PALS throughout an immune response. Though it is possible that true-memory cells possess an advantage in acquiring particular signals in the RP/MZ, it is also likely that the proper programming is a necessity to successfully reach those signals. As mentioned earlier, the presence of naïve and HP-memory subsets in the PALS indicates that there may be signals within the region necessary for memory formation. Some of these signals could be due to cytokines or cellular interactions with DCs. In recent years, it has been demonstrated by multiple groups that KLRG-1 and IL-7R expression characterize different populations of memory-track or effector cells [29-31, 44]. Termed SLEC or MPEC, it is the idea that MPECs ($KLRG\text{-}1^{lo}/IL\text{-}7R^{hi}$) have higher tendencies to form stable memory cells than SLECs ($KLRG\text{-}1^{hi}/IL\text{-}7R^{lo}$) [31]. When both effector populations were adoptively transferred into new hosts, the MPECs preferentially give rise to a stable memory pool [29, 31]. It is also of note that shortening the immune response and inflammation (i.e. treatment with antibiotics) decreases the number of SLECs but does not alter MPEC survival, also suggesting that dedication to the memory pathway might be programmed early [30, 31]. Combining these trends with our findings, staining for gradients of these markers in our immune response model may reveal the anatomical location of $CD8^+$ T cell memory formation in the PALS.

Both naïve and HP-memory subsets contain significant populations that remain within the PALS throughout the infection, and as different as their effector potentials are, they share the principle property of having never been exposed to antigen. In contrast, true-memory cells, in each case shown, traffic quickly into the RP/MZ, leaving few

lingering cells within the PALS. The localization patterns seen through histology correlate with the results of Joshi, et. al that show KLRG-1 upregulation (SLECs) occurs around days 4-5 [31], also the approximate period that true-memory cells begin to polarize to the RP/MZ. They also demonstrate that IL-7R levels on SLECs decrease by days 6-8, correlating with the most evident true-memory localization pattern on days 8-10 [29, 30]. Taken together, optimizing future immunofluorescence stainings for the key markers KLRG-1 and IL7-R could reveal a gradient in staining, depicting the maturation of cells localized in the PALS into either SLECs or MPECs as they migrate to the RP/MZ. In addition, combining these stains with T cell receptor tetramers can also reveal whether DCs play a role in the late phase localization of non-antigen-experienced and antigen-specific effector cells as well. A gradient that displays PALS-localized cells as MPECs and those in the RP/MZ as SLECs can pinpoint the probable anatomical location of seeding the memory compartment, revealing another piece to the puzzle of immunological memory.

Figures 3-8, in full, are reprints of the material as they appears in a manuscript currently in review at The Journal of Immunology, with the running title "Memory-like $CD8^+$ T cells generated during homeostatic proliferation defer to antigen-experienced memory cells." Authors are as follows: Kitty P. Cheung, Edward Yang, and Ananda W. Goldrath. The thesis author was the second author of this paper.

MATERIALS AND METHODS

Mice and adoptive transfers

All mouse work was performed in an AAALAC accredited facility according to the UCSD Institutional Animal Care and Use Guidelines. C57BL/6J (B6) mice were obtained from The Jackson Laboratory and bred in our facility along with CD45.1 and CD45.1.2 congenic mice on a B6 background. OT-I $RAG^{-/-}$ TCR-transgenic mice (CD45.1 or CD45.1.2) express a Vα2Vβ5 TCR heterodimer that recognizes a peptide derived from $ovalbumin_{(257–264)}$ (OVAp) presented by $H\text{-}2K^b$.

To generate HP-memory populations, 10^6 $CD44^{lo}$ OT-I cells (CD45.1) were sorted and adoptively transferred into B6 hosts rendered lymphopenic by sub-lethal irradiation (600rads) 24 h prior. Cells were allowed to undergo homeostatic proliferation for at least 30 days before subsequent transfers. For generation of true-memory, 10^6 OT-I (CD45.1.2) cells were adoptively transferred into naïve mice and infected with 5000 cfu Lm.OVA i.v.; 30 days were allowed to pass before subsequent transfers. Before the second adoptive transfer into naïve B6 mice, lymphocytes from spleen and lymph nodes were pooled and depleted of B and $CD4^+$ T cells (MACS). 1×10^5 - 8×10^5 cells were transferred per mouse unless otherwise specified; similar results were obtained for this range. Mice were re-challenged with 10^5 cfu Lm.OVA, immunized with 100ug OVAp/50ug LPS, or left uninfected. Where indicated, lymphocytes from pooled spleen and lymph nodes were labeled with CFSE (10μM final concentration, Molecular Probes) for 10 min at 37°C in PBS 0.1% BSA.

To inhibit CD62L-mediated entry into lymph nodes, 200 mg of anti-CD62L (MEL-14) was administered i.p ~4 h before adoptive transfer of memory cells. The next day 200 mg of antibody was administered i.p ~4 h before infection and thereafter each day. Rat IgG2a κ isotype or PBS was administered concurrently to control mice with similar results to untreated hosts. For cytokine complexes, IL-7 was pre-complexed with an anti-IL-7 mAb (500-M07 PeproTech) and IL-15 was pre-complexed with its soluble IL-15-receptor-a as previously described and administered i.p on days 3-7 of infection.

Lymphocytes isolated from lung and liver, as previously described with minor modifications. Mice were euthanized with CO_2 and perfused with PBS. Following collagenase digestion, cells were resuspended in HBSS, 5mM EDTA, and 2% BGS, and layered on Ficoll-Paque Plus solution (Amersham Bioscience) and separated according to manufacturer's instructions. Intraepithelial lymphocytes (IEL) were isolated as previously described with a modified protocol. After incubation with 1mM dithioerythritol, tissue was incubated at 37^{o}C with HBSS, 1.3mM EDTA for 30 min and layered over Ficoll.

Flow Cytometry

Following secondary challenge, single cell suspensions were prepared from spleen and lymph node lysates. Fc receptors were first blocked with unconjugated mouse antibody to CD32/16 (2.4G2). The following antibodies were used for phenotypic analysis: CD44 (IM7), CD62L (Mel-14), CD122 (TM-β1), CD127 (A7R34), LY6C (AL-2), CD43 (1B11), CXCR3 (R&D Cat# FAB1585P), CD27 (LG.759), CD49d (R1-2), KLRG1 (2F1), PD-1 (J43), CD132 (4G3), CD45.1 (A20), CD45.2 (104), and CD8α (53-6.7). All

antibodies are available commercially from Ebioscience or BD Pharmingen unless otherwise noted. To detect apoptosis, APC-conjugated annexin V/annexin buffer (Invitrogen) and 7-AAD (Invitrogen) were used. TUNEL staining was performed using the FragEL DNA fragmentation detection kit (Calbiochem) according to manufacturer's instructions. In short, cells were stained with surface antibodies then fixed in PBS with 1% paraformaldehyde. Following a wash in PBS and 0.2% Tween, fluorescent TdT mix was added and incubated for 1.5 h. To measure in-vivo proliferation, 1 mg BrdU (Sigma-Aldrich) was injected i.p into mice 15 h prior to sacrifice on indicated days. Splenocytes or lymph node cells were stained according to instructions from the BrdU Flow kit (BD Biosciences). All samples were run on BD's FACSCalibur or FACSAria. FlowJo software (TreeStar) was used for analysis.

mRNA Array

SuperArray®'s qPCR array (Cat No. PAMM-022) was used to compare the relative levels of cDNA between HP- and true-memory OT-I cells 6 days post infection from sorted pooled spleen cells. mRNA was extracted using TRIzol (Invitrogen) and cDNA was generated using the RT^2 First Strand Kit (Superarray). Primers for mouse CXCR5 and CCR7 and the RT^2 SYBR Green/ROX PCR Master mix were obtained from SuperArray. For each set of triplicates, the mean value of each gene was calculated using the $\Delta\Delta C_t$ method in comparison with the housekeeping gene.

Immunofluorescence

Freshly harvested tissues were soaked in 30% sucrose overnight and embedded in OCT. 6μm thick tissue sections were cut and fixed in acetone (-20°C). Sections were blocked in a solution of 10% bovine serum albumin, 2.5% normal goat serum, 2.5% normal donkey serum, and fish scale gelatin. Tissue sections were then incubated with combinations of conjugated anti-mouse CD45.1, anti-rat Thy1.1/CD90 (OX-7), anti-mouse B220 (RA3-GB2), anti-mouse CD8a, anti-mouse CD4 (GK1.5) or anti-mouse CD11c (N418) followed by incubation with secondary mAb Alexa Fluor 546 streptavidin. Sections were mounted using Invitrogen ProLong Gold antifade reagent. Images were taken with an Olympus FV1000 confocal microscope with 5 laser lines at wavelengths of 405, 458, 488, 515, 543, and 647nm, using 10X and 20X air objectives. Images were analyzed using ImageJ.

REFERENCES

1. Harty, J.T. and V.P. Badovinac, *Shaping and reshaping CD8+ T-cell memory.* Nat Rev Immunol, 2008. **8**(2): p. 107-19.
2. Bradley, L.M., L. Haynes, and S.L. Swain, *IL-7: maintaining T-cell memory and achieving homeostasis.* Trends Immunol, 2005. **26**(3): p. 172-6.
3. Scholer, A., S. Hugues, A. Boissonnas, L. Fetler, and S. Amigorena, *Intercellular adhesion molecule-1-dependent stable interactions between T cells and dendritic cells determine CD8+ T cell memory.* Immunity, 2008. **28**(2): p. 258-70.
4. Kaech, S.M., S. Hemby, E. Kersh, and R. Ahmed, *Molecular and functional profiling of memory CD8 T cell differentiation.* Cell, 2002. **111**(6): p. 837-51.
5. Murali-Krishna, K., J.D. Altman, M. Suresh, D.J. Sourdive, A.J. Zajac, J.D. Miller, J. Slansky, and R. Ahmed, *Counting antigen-specific CD8 T cells: a reevaluation of bystander activation during viral infection.* Immunity, 1998. **8**(2): p. 177-87.
6. Agarwal, S. and A. Rao, *Modulation of chromatin structure regulates cytokine gene expression during T cell differentiation.* Immunity, 1998. **9**(6): p. 765-75.
7. Veiga-Fernandes, H., U. Walter, C. Bourgeois, A. McLean, and B. Rocha, *Response of naive and memory CD8+ T cells to antigen stimulation in vivo.* Nat Immunol, 2000. **1**(1): p. 47-53.
8. Kaech, S.M. and R. Ahmed, *Memory CD8+ T cell differentiation: initial antigen encounter triggers a developmental program in naive cells.* Nat Immunol, 2001. **2**(5): p. 415-22.
9. Masopust, D., S.M. Kaech, E.J. Wherry, and R. Ahmed, *The role of programming in memory T-cell development.* Curr Opin Immunol, 2004. **16**(2): p. 217-25.
10. Kaech, S.M., E.J. Wherry, and R. Ahmed, *Effector and memory T-cell differentiation: implications for vaccine development.* Nat Rev Immunol, 2002. **2**(4): p. 251-62.
11. Bevan, M.J. and P.J. Fink, *The CD8 response on autopilot.* Nat Immunol, 2001. **2**(5): p. 381-2.
12. Goldrath, A.W., P.V. Sivakumar, M. Glaccum, M.K. Kennedy, M.J. Bevan, C. Benoist, D. Mathis, and E.A. Butz, *Cytokine requirements for acute and Basal homeostatic proliferation of naive and memory CD8+ T cells.* J Exp Med, 2002. **195**(12): p. 1515-22.
13. Goldrath, A.W., *Maintaining the status quo: T-cell homeostasis.* Microbes Infect, 2002. **4**(5): p. 539-45.
14. Cho, B.K., V.P. Rao, Q. Ge, H.N. Eisen, and J. Chen, *Homeostasis-stimulated proliferation drives naive T cells to differentiate directly into memory T cells.* J Exp Med, 2000. **192**(4): p. 549-56.
15. Goldrath, A.W., C.J. Luckey, R. Park, C. Benoist, and D. Mathis, *The molecular program induced in T cells undergoing homeostatic proliferation.* Proc Natl Acad Sci U S A, 2004. **101**(48): p. 16885-90.
16. Hamilton, S.E., M.C. Wolkers, S.P. Schoenberger, and S.C. Jameson, *The generation of protective memory-like CD8+ T cells during homeostatic proliferation requires CD4+ T cells.* Nat Immunol, 2006. **7**(5): p. 475-81.

17. Tan, J.T., E. Dudl, E. LeRoy, R. Murray, J. Sprent, K.I. Weinberg, and C.D. Surh, *IL-7 is critical for homeostatic proliferation and survival of naive T cells.* Proc Natl Acad Sci U S A, 2001. **98**(15): p. 8732-7.
18. Zammit, D.J. and L. Lefrancois, *Dendritic cell-T cell interactions in the generation and maintenance of CD8 T cell memory.* Microbes Infect, 2006. **8**(4): p. 1108-15.
19. Heath, W.R., G.T. Belz, G.M. Behrens, C.M. Smith, S.P. Forehan, I.A. Parish, G.M. Davey, N.S. Wilson, F.R. Carbone, and J.A. Villadangos, *Cross-presentation, dendritic cell subsets, and the generation of immunity to cellular antigens.* Immunol Rev, 2004. **199**: p. 9-26.
20. Pozzi, L.A., J.W. Maciaszek, and K.L. Rock, *Both dendritic cells and macrophages can stimulate naive CD8 T cells in vivo to proliferate, develop effector function, and differentiate into memory cells.* J Immunol, 2005. **175**(4): p. 2071-81.
21. Khanna, K.M. and L. Lefrancois, *Geography and plumbing control the T cell response to infection.* Immunol Cell Biol, 2008. **86**(5): p. 416-22.
22. Khanna, K.M., J.T. McNamara, and L. Lefrancois, *In situ imaging of the endogenous CD8 T cell response to infection.* Science, 2007. **318**(5847): p. 116-20.
23. Mempel, T.R., S.E. Henrickson, and U.H. Von Andrian, *T-cell priming by dendritic cells in lymph nodes occurs in three distinct phases.* Nature, 2004. **427**(6970): p. 154-9.
24. Williams, M.A. and M.J. Bevan, *Effector and memory CTL differentiation.* Annu Rev Immunol, 2007. **25**: p. 171-92.
25. Khoruts, A., and J. M. Fraser, *A causal link between lymphopenia and autoimmunity.* Immunology Letters, 2005. **98**: p. 23-31.
26. Dummer, W., A.G. Niethammer, R. Baccala, B.R. Lawson, N. Wagner, R.A. Reisfeld, and A.N. Theofilopoulos, *T cell homeostatic proliferation elicits effective antitumor autoimmunity.* J Clin Invest, 2002. **110**(2): p. 185-92.
27. Selin, L.K., M.Y. Lin, K.A. Kraemer, D.M. Pardoll, J.P. Schneck, S.M. Varga, P.A. Santolucito, A.K. Pinto, and R.M. Welsh, *Attrition of T cell memory: selective loss of LCMV epitope-specific memory CD8 T cells following infections with heterologous viruses.* Immunity, 1999. **11**(6): p. 733-42.
28. McNally, J.M., C.C. Zarozinski, M.Y. Lin, M.A. Brehm, H.D. Chen, and R.M. Welsh, *Attrition of bystander CD8 T cells during virus-induced T-cell and interferon responses.* J Virol, 2001. **75**(13): p. 5965-76.
29. Kaech, S.M., J.T. Tan, E.J. Wherry, B.T. Konieczny, C.D. Surh, and R. Ahmed, *Selective expression of the interleukin 7 receptor identifies effector CD8 T cells that give rise to long-lived memory cells.* Nat Immunol, 2003. **4**(12): p. 1191-8.
30. Kaech, S.M. and E.J. Wherry, *Heterogeneity and cell-fate decisions in effector and memory CD8+ T cell differentiation during viral infection.* Immunity, 2007. **27**(3): p. 393-405.
31. Joshi, N.S., W. Cui, A. Chandele, H.K. Lee, D.R. Urso, J. Hagman, L. Gapin, and S.M. Kaech, *Inflammation directs memory precursor and short-lived effector*

CD8(+) T cell fates via the graded expression of T-bet transcription factor. Immunity, 2007. **27**(2): p. 281-95.

32. Muller, G., U.E. Hopken, and M. Lipp, *The impact of CCR7 and CXCR5 on lymphoid organ development and systemic immunity.* Immunol Rev, 2003. **195**: p. 117-35.
33. Sarkar, S., V. Kalia, W.N. Haining, B.T. Konieczny, S. Subramaniam, and R. Ahmed, *Functional and genomic profiling of effector CD8 T cell subsets with distinct memory fates.* J Exp Med, 2008. **205**(3): p. 625-40.
34. Strauss-Ayali, D., S.M. Conrad, and D.M. Mosser, *Monocyte subpopulations and their differentiation patterns during infection.* J Leukoc Biol, 2007. **82**(2): p. 244-52.
35. Prlic, M., L. Lefrancois, and S.C. Jameson, *Multiple choices: regulation of memory CD8 T cell generation and homeostasis by interleukin (IL)-7 and IL-15.* J Exp Med, 2002. **195**(12): p. F49-52.
36. Kedl, R.M., J.W. Kappler, and P. Marrack, *Epitope dominance, competition and T cell affinity maturation.* Curr Opin Immunol, 2003. **15**(1): p. 120-7.
37. Haynes, N.M., C.D. Allen, R. Lesley, K.M. Ansel, N. Killeen, and J.G. Cyster, *Role of CXCR5 and CCR7 in follicular Th cell positioning and appearance of a programmed cell death gene-1high germinal center-associated subpopulation.* J Immunol, 2007. **179**(8): p. 5099-108.
38. Bousso, P. and E. Robey, *Dynamics of CD8+ T cell priming by dendritic cells in intact lymph nodes.* Nat Immunol, 2003. **4**(6): p. 579-85.
39. Badovinac, V.P., K.A. Messingham, A. Jabbari, J.S. Haring, and J.T. Harty, *Accelerated CD8+ T-cell memory and prime-boost response after dendritic-cell vaccination.* Nat Med, 2005. **11**(7): p. 748-56.
40. Lappin, M.B., J.M. Weiss, V. Delattre, B. Mai, H. Dittmar, C. Maier, K. Manke, S. Grabbe, S. Martin, and J.C. Simon, *Analysis of mouse dendritic cell migration in vivo upon subcutaneous and intravenous injection.* Immunology, 1999. **98**(2): p. 181-8.
41. Laugel, B., J.M. Boulter, N. Lissin, A. Vuidepot, Y. Li, E. Gostick, L.E. Crotty, D.C. Douek, J. Hemelaar, D.A. Price, B.K. Jakobsen, and A.K. Sewell, *Design of soluble recombinant T cell receptors for antigen targeting and T cell inhibition.* J Biol Chem, 2005. **280**(3): p. 1882-92.
42. Boulter, J.M. and B.K. Jakobsen, *Stable, soluble, high-affinity, engineered T cell receptors: novel antibody-like proteins for specific targeting of peptide antigens.* Clin Exp Immunol, 2005. **142**(3): p. 454-60.
43. Subbramanian, R.A., C. Moriya, K.L. Martin, F.W. Peyerl, A. Hasegawa, A. Naoi, H. Chhay, P. Autissier, D.A. Gorgone, M.A. Lifton, K. Kuus-Reichel, J.E. Schmitz, N.L. Letvin, and M.J. Kuroda, *Engineered T-cell receptor tetramers bind MHC-peptide complexes with high affinity.* Nat Biotechnol, 2004. **22**(11): p. 1429-34.
44. Lefrancois, L. and A.L. Marzo, *The descent of memory T-cell subsets.* Nat Rev Immunol, 2006. **6**(8): p. 618-23.